Preprint
UCRL-JC-152983

Quiescent Double Barrier H-Mode Plasmas in the DIII-D Tokamak

K.H. Burrell, M. E. Austin, D. P. Brennan, J. C. DeBoo,
E. J. Doyle, C. Fenzi, C. Fuchs, P. Gohil, C. M.Greenfield
R. J. Groebner, L. L. Lao, T. C. Luce, M. A. Makowski,
G. R. McKee, R. A. Moyer, C. C. Petty, M. Porkolab, C. L Rett
T. L. Rhodes, J. C. Rost, B. W. Stallard, E. J. Strait, E. J. Synakows
M. R. Wade, J. G. Watkins, W. P. West

This article was submitted to: 42nd Annual Meeting of the APS Division of Plasma Physics, Quebec City, Canada 11/23-11/27/00

November 1, 2000

This work was performed under the auspices of the United States Department of Energy by the University of California, Lawrence Livermore National Laboratory under contract No. W-7405-Eng-48.

GA–A23552

QUIESCENT DOUBLE BARRIER H–MODE PLASMAS IN THE DIII–D TOKAMAK

by
K.H. BURRELL, M.E. AUSTIN,* D.P. BRENNAN, J.C. DeBOO, E.J. DOYLE,† C. FENZI,‡ C. FUCHS,# P. GOHIL, C.M. GREENFIELD, R.J. GROEBNER, L.L. LAO, T.C. LUCE, M.A. MAKOWSKI,△ G.R. McKEE,‡ R.A. MOYER,¶ C.C. PETTY, M. PORKOLAB,§ C.L. RETTIG,† T.L. RHODES,† J.C. ROST,§ B.W. STALLARD,△ E.J. STRAIT, E.J. SYNAKOWSKI,◊ M.R. WADE,∞ J.G. WATKINS,□ and W.P. WEST

This is a preprint of an invited paper presented at the 42nd Annual Meeting of the Division of Plasma Physics, November 23–27, 2000 in Quebec City, Canada, and to be published in *Phys. Plasmas.*

*University of Texas, Austin, Texas.
†University of California, Los Angeles, California.
‡University of Wisconsin, Madison, Wisconsin.
#Max Planck Institut für Plasmaphysik, Garching, Germany.
△Lawrence Livermore National Laboratory, Livermore, California.
¶University of California, San Diego, California.
§Massachusetts Institute of Technology, Cambridge, Massachusetts.
◊Princeton Plasma Physics Laboratory, Princeton, New Jersey.
∞Oak Ridge National Laboratory, Oak Ridge, Tennessee.
□Sandia National Laboratories, Albuquerque, New Mexico.

Work supported by
the U.S. Department of Energy under Contract Nos.
DE-AC03-99ER54463, W-7405-ENG-48, DE-AC02-76CH03073, DE-AC05-00OR22725,
DE-AC04-94AL85000, and Grant Nos. DE-FG03-97ER54415, DE-FG03-86ER53225,
DE-FG03-96ER54373, DE-FG03-95ER54294, and DE-FG02-94ER54235

GA PROJECT 30033
NOVEMBER 2000

ABSTRACT

High confinement (H–mode) operation is the choice for next-step tokamak devices based either on conventional or advanced tokamak physics. This choice, however, comes at a significant cost for both the conventional and advanced tokamaks because of the effects of edge localized modes (ELMs). ELMs can produce significant erosion in the divertor and can affect the beta limit and reduced core transport regions needed for advanced tokamak operation. Experimental results from DIII-D [J.L. Luxon, et al., Plasma Phys. and Contr. Nucl. Fusion Research 1986 (International Atomic Energy Agency, Vienna, 1987) Vol. I, p. 159] this year have demonstrated a new operating regime, the quiescent H-mode regime, which solves these problems. We have achieved quiescent H-mode operation which is ELM-free and yet has good density and impurity control. In addition, we have demonstrated that an internal transport barrier can be produced and maintained inside the H-mode edge barrier for long periods of time (>3.5 seconds or >25 energy confinement times τ_E), yielding a quiescent double barrier regime. By slowly ramping the input power, we have achieved $\beta_N H_{89} = 7$ for up to 5 times the τ_E of 150 ms. The $\beta_N H_{89}$ values of 7 substantially exceed the value of 4 routinely achieved in standard ELMing H-mode. The key factors in creating the quiescent H-mode operation are neutral beam injection in the direction opposite to the plasma current (counter injection) plus cryopumping to reduce the density. Density and impurity control in the quiescent H-mode is possible because of the presence of an edge magnetic hydrodynamic (MHD) oscillation, the edge harmonic oscillation, which enhances the edge particle transport while leaving the energy transport unaffected.

I. INTRODUCTION

Because of its superior energy confinement, high confinement (H-mode) operation is the choice for next step tokamak devices based either on conventional [1] or advanced tokamak [2,3] physics. This choice, however, comes at a significant cost for both the conventional and advanced tokamaks because of the effects of edge localized modes (ELMs). The standard view is that ELMing H-mode operation is required for density and impurity control. However, the ELMs produce pulsed divertor heat and particle loads which can lead to rapid erosion of the divertor plates [4]. In addition, for the advanced tokamak, giant ELMs couple to core magnetohydrodynamic (MHD) modes (e.g. neo-classical tearing modes) and thus reduce the beta limit. Furthermore, giant ELMs can destroy the reduced transport core which is needed for the profile optimization required for advanced tokamak operation [5]. Experimental results from DIII-D [6] this year have demonstrated a new operating regime which solves these problems. We have achieved quiescent H-mode operation which is ELM-free and yet has good density and impurity control. In addition, we have demonstrated that an internal transport barrier can be produced and maintained inside the H-mode edge barrier, producing an operating regime dubbed the quiescent double barrier (QDB) regime. The QDB plasmas have significantly improved plasma performance relative to that of standard ELMing H-mode.

The key factors in creating the quiescent H-mode operation are neutral beam injection in the direction opposite to the plasma current (counter injection) plus cryopumping to reduce the density. These have allowed long pulse, ELM-free operation with constant density and radiated power levels for periods up to 3.5 seconds or about 25 global energy confinement times τ_E. There is no known plasma physics limitation which would prevent this quiescent operation from being extended to steady state. The duration in present experiments was limited by the choice of plasma current flat top and the choice of neutral beam pulse length. The duration of the reduced core transport exceeds that of the quiescent H-mode edge, since the core transport reduction begins before the ELMs go away and the quiescent H-mode is established. Normalized performance in terms of β_N and H_{89} improves with increasing neutral beam input power. Here $\beta_N = \beta/(I/aB_T)$ is the normalized beta [2,3] in %m·T/MA and H_{89} is the confinement enhancement factor relative to the ITER89P scaling [1]. By slowly ramping the power, we have achieved $\beta_N H_{89} = 7$ for up to 5 τ_E. The $\beta_N H_{89}$ values of 7 substantially exceed the value of 4 routinely achieved in standard ELMing H-mode.

Density and impurity control in the quiescent H-mode is possible because of the presence of an edge MHD oscillation, the edge harmonic oscillation, which enhances the

edge particle transport while leaving the energy transport unaffected. The qualitative behavior induced by this mode is similar to that reported for the quasi-coherent mode in enhanced D_α (EDA) operation in the C-Mod tokamak [7-9]; however, the details of the two modes are quite different.

Initially, reduced core transport plasmas in tokamaks were seen only in transient conditions. This led to questions of their relevance to next-step devices and reactors which require, at a minimum, long-pulse operation. One of the goals of DIII-D research over the past five years has been to extend the duration of such plasmas. With the QDB regime, we have pushed the duration to >3.5 seconds or about 25 τ_E. It now appears that the only obstacle to operating such plasmas in steady-state is the need for sufficient current drive to keep minimum q above one.

II. QUIESCENT H-MODE EDGE

A. Basic nature of quiescent H-mode

Figure 1 illustrates the basic behavior of quiescent H-mode shots run during the 2000 campaign on DIII-D. After an initial ELMing phase, the bursts on the divertor D_α signal disappear, giving a quiescent phase, which is the source of the name for this operating regime. Unlike the monotonic increase seen in standard ELM-free H-mode, the density [Fig. 1(b)] and radiated power [Fig. 1(g)] are essentially constant during the quiescent phase. This indicates that the particle transport at the plasma edge is rapid enough to provide density and impurity control. As is seen in Fig. 1(f), the nature of the oscillations detected by the magnetic pickup loops changes when the ELMs cease from a bursting behavior to a much more continuous oscillation. This is the edge harmonic oscillation which will be discussed extensively later in the paper. Our data indicate that the presence of this oscillation is what provides the enhanced edge particle transport. Although the edge harmonic oscillation gives enhanced particle transport, it has little effect on the

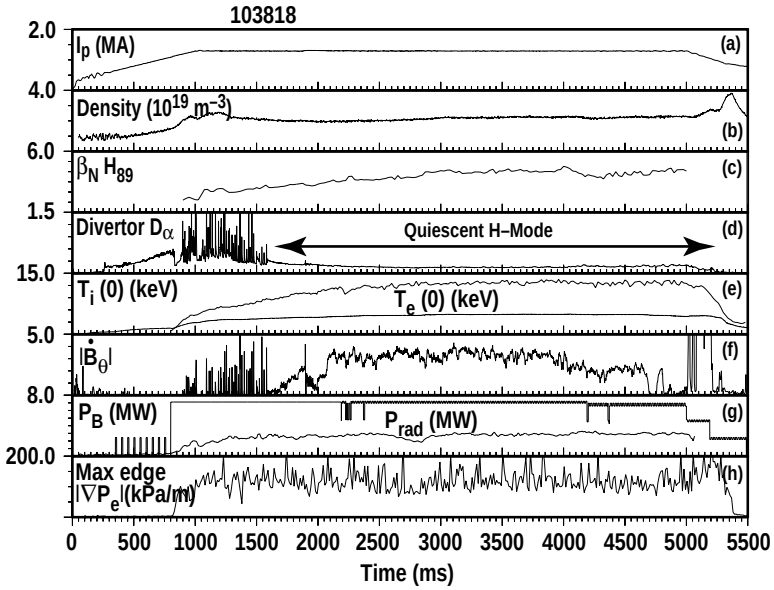

Fig. 1. Time history of a quiescent H-mode shot. (a) plasma current, (b) line-averaged density, (c) product of normalized beta β_N and energy confinement time enhancement factor H_{89}, (d) divertor D_α emission, (e) central ion and electron temperature, (f) $\dot{B}_\theta$ from magnetic probe, (g) total injected neutral beam power and total radiated power, (h) maximum edge electron pressure gradient determined from a hyperbolic tangent fit to the electron pressure measured by Thomson scattering. Toroidal field is 2.0 T.

energy transport. The edge temperature and pressure gradients in the quiescent H-mode are as large as those in ELMing H-mode. The global energy confinement time in these quiescent phases is at or above the standard H-mode level. Combining the quiescent H-mode edge with the reduced transport core to achieve high performance is discussed in Section III.

Figure 1 also illustrates that the quiescent H-mode can operate for long periods of time. This particular shot is ELM-free for about 3.5 seconds or about 25 τ_E. The quiescent phase terminates only because the plasma current and neutral beam power were programmed to ramp down at 5.0 seconds into the shot. As far as is known, there is no plasma physics reason why the quiescent phase cannot be extended indefinitely.

Although most of the shots in the 2000 campaign have an ELMing phase prior to the quiescent phase, this sequence does not always occur. During the 1999 campaign, we ran shots which were limited on the centerpost of the vacuum vessel for the first 1800 ms of the discharge. The plasma was then changed to a diverted, pumping shape. In these cases, the quiescent phase sometimes arose directly out of the standard ELM-free phase just after the L to H transition.

B. Conditions for quiescent H-mode

Quiescent H-mode plasmas were discovered in DIII-D in 1999 when we combined counter-injection with cryopumping to lower the plasma density [10,11]. In experiments conducted so far, we need neutral beam powers above about 3.7 MW to access this operating regime. Line averaged densities are typically in the range of 2 to 3×10^{19} m^{-3} while the local density at the top of the H-mode edge pedestal is around 1 to 2×10^{19} m^{-3}. For comparison, line-averaged and pedestal densities are both around 6×10^{19} m^{-3} in unpumped ELMing H-mode at the same current. The exact density boundary has not been established as a function of the other plasma parameters. However, data clearly show that increased gas puffing or pellet injection into established quiescent plasmas can lead to the destruction of the edge harmonic oscillation and a return of the ELMs. The quiescent phase can be re-established once the edge density perturbation decays. Quiescent H-modes are typically operated with no extra particle fueling beyond that provided by the neutral beam injection. These results suggest that the role of cryopumping in creating quiescent H-mode is control of the edge plasma or neutral density.

A third necessary condition for robust quiescent H-mode operation is a sufficiently large distance between the plasma edge and the vacuum vessel wall on the low toroidal field side of the discharge. Typically, distances of 10 cm are sufficient. This is probably related to use of counter neutral beam injection. For counter injection, there are a significant number of neutral beam produced fast ions which exist outside the plasma edge. It

appears that interaction of these particles with the vessel wall is detrimental to quiescent operation. Exactly why this interaction is detrimental is not known. One possibility is that extra gas evolved from the wall owing to this interaction affects the quiescent phase the same way that an extra gas puff does.

Single-null divertor configurations were used in all of the quiescent H-mode experiments to date. Double-null operation has yet to be attempted, since cryopumping is much less efficient in double-null plasmas given the present cryopump configuration in DIII-D. The direction of the ion ∇B drift relative to the divertor X-point does not matter; quiescent operation has been seen in both cases. We have seen quiescent H-modes over entire range of triangularity ($0.16 \le \delta \le 0.75$) and q_{95} ($3.7 \le q_{95} \le 4.6$) explored to date. Most of our work has been done with plasma current I_p in the range $1.2 \le I_p$ (MA) ≤ 1.6 and toroidal field B_T in the range $1.8 \le B_T$ (T) ≤ 2.1 with neutral beam powers up to 13.5 MW. We also have quiescent H-mode examples at 0.67 MA and 0.95 T.

C. Steep edge gradients

After the ELMs cease, the divertor D_α trace in Fig. 1(d) superficially looks like a return to L-mode; accordingly, it is important to establish that the quiescent phase truly is an H-mode. As is shown in Fig. 2, the edge density and temperature gradients in the quiescent phase are as steep as the ones in the ELMing phase of the discharge. Since it is the edge transport barrier which is the *sine qua non* of the H-mode, the quiescent phase is indeed H-mode. The continuation of the steep edge gradients into the quiescent H-mode phase is also illustrated in Fig. 1(h) where we see that the maximum edge electron pressure gradient does not change when the ELMs cease and the quiescent phase begins.

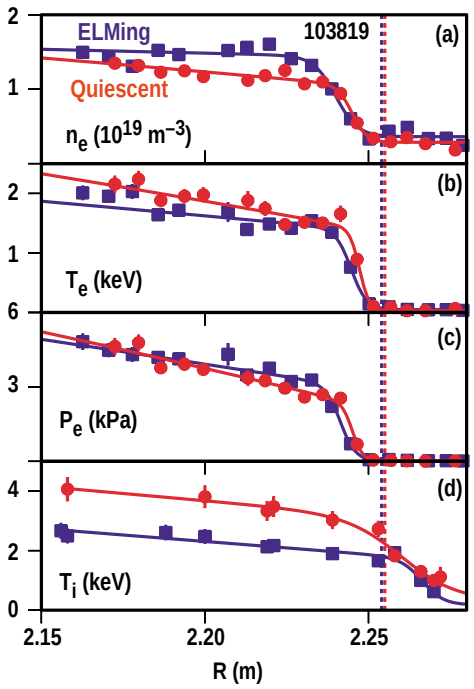

Fig. 2. Comparison of edge profiles for the ELMing and quiescent phases of a discharge similar to that in Fig. 1 showing that the edge gradients are quite similar in both phases. (a) Electron density (b) electron temperature, (c) electron pressure, and (d) ion temperature profile. Electron measurements are from Thomson scattering while the ion measurement is from charge exchange spectroscopy using C^{6+}. Square symbols show the ELMing phase while round symbols show the quiescent phase. Dashed vertical line shows separatrix location.

D. Particle flux enhanced by edge harmonic oscillation

A key feature of the quiescent H-mode is the constant density and impurity levels in the absence of ELMs. This is quite an astonishing result, given the worldwide observation of continuous density and radiated power increase in standard ELM-free H-modes and VH-modes [12]. This increase in standard ELM-free H-mode and VH-modes is due to the very low particle flux out of these plasmas. Since the quiescent H-mode does not exhibit this increase, the outward particle flux must be substantially larger. A fundamental question, then, is how this comes about.

As is shown in Fig. 3, the onset of the edge harmonic oscillation coincides with an increase in the D_α radiation from the entire divertor region. This demonstrates that the edge oscillation increases the flux of particles out of the main discharge and into the divertor. In addition, as is shown in Fig. 3(e), the line averaged density begins to decrease at the time that the edge harmonic oscillation starts. The density had been rising slowly

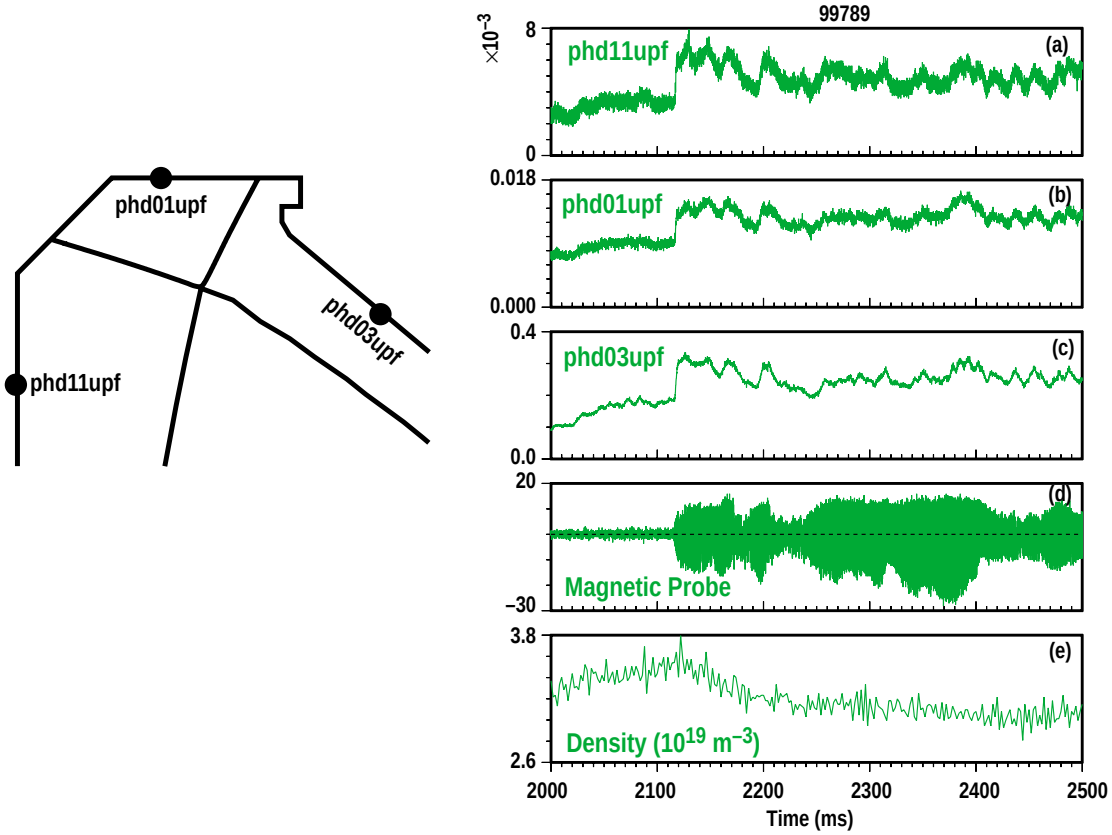

Fig. 3. Time history of signals from an upper single-null divertor discharge showing (a-c) divertor D_α radiation from three photodetection system viewing different points in the divertor region of DIII-D, (d) signal from midplane magnetic probe showing the edge harmonic oscillation (e) line averaged density. When the edge harmonic oscillation starts, the D_α emission from all regions of the divertor increases. The cartoon shows where the D_α chord views; each chord views from the bottom of the vessel to the spot indicated on the vessel ceiling.

before that time. Together, these observations show clearly that it is the edge harmonic oscillation which provides the enhanced particle flux which allows the density and impurity control.

Measurements with Langmuir probes in the scrape-off layer at the plasma midplane [13] and on the divertor plates [14] both show the presence of the edge harmonic oscillation. The ion saturation current to the probes shows the same harmonic frequency structure shown in Fig. 4 for the magnetic probes. The divertor plate probes which are in contact with the scrape-off layer plasma are the ones which show the oscillation. Probes in the private flux region on the other side of the separatrix do not show it. These measurements demonstrate directly that the particle flux to the divertor plate is also affected by the edge oscillation.

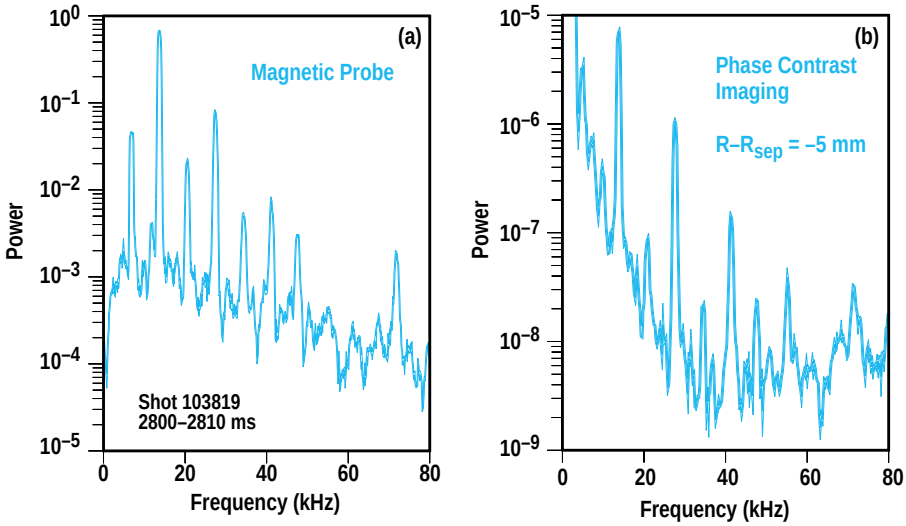

Fig. 4. Autopower spectrum of the edge harmonic oscillation as detected on (a) a midplane magnetic probe and (b) the phase contrast imaging system at a point 5 mm inside the separatrix. Phase contrast imaging is sensitive to density fluctuations with primarily radial wavenumbers. Both diagonstics show peaks at the same frequencies and both show the multiple harmonics characteristic of this oscillation.

E. Nature of the edge harmonic oscillation

Although it was first seen on the magnetic probes, the edge harmonic oscillation also has density and temperature fluctuations associated with it. Density fluctuations have been seen using beam emission spectroscopy (BES) [15], reflectometry [16,17], FIR scattering [18] and phase contrast imaging (PCI) [19] while the temperature fluctuations have been seen on the electron cyclotron emission (ECE) diagnostic [20]. As is illustrated in Fig. 4, the density and magnetic oscillations both show multiple harmonics in the range of 1 to 10. Because the oscillation is weaker 3-4 cm inside the separatrix where the electron cyclotron emission is black-body, we can only detect the fundamental and the first

one or two harmonics on the temperature oscillation above the photon statistics noise in the ECE system. Analysis with the DIII-D magnetic probe array shows that each distinct frequency has its associated toroidal mode number n. In other words, the fundamental frequency f has an n=1 toroidal mode number, 2f has an n=2 toroidal mode number, etc. If one looks at the actual oscillation on the magnetic probes, for example, it is clear that the oscillation is periodic but not sinusoidal. The multiple harmonics/multiple n numbers are simply the Fourier harmonics needed to describe such a non-sinusoidal oscillation. The density, temperature and magnetic oscillations are highly coherent with each other at each of the harmonics. The change in phase with toroidal angle detected by the magnetic probes shows that the edge oscillation propagates in the same direction the neutral beams.

The mix of Fourier harmonics involved in the edge harmonic oscillation is variable, as is illustrated in Fig. 5. The mix can vary from shot to shot or even within one shot. Surprisingly, the measured edge pressure gradients do not change significantly even when the mix of toroidal harmonics changes as long as the oscillation is present. When the edge harmonic oscillation ceases, the plasma returns to standard ELM-free conditions and the edge density rises. ELMs follow within roughly 100 ms or less. Such a cessation sometimes occurs, for example, when we deliberately decrease the gap between the plasma and the wall in order to scan the plasma edge across the various edge diagnostics. Typically, there is a delay of 50 to 100 ms between the time of minimum gap and the cessation. There are other cases where the edge harmonic oscillation spontaneously ceases for 10's of milliseconds for reasons that are not yet understood. These are typically

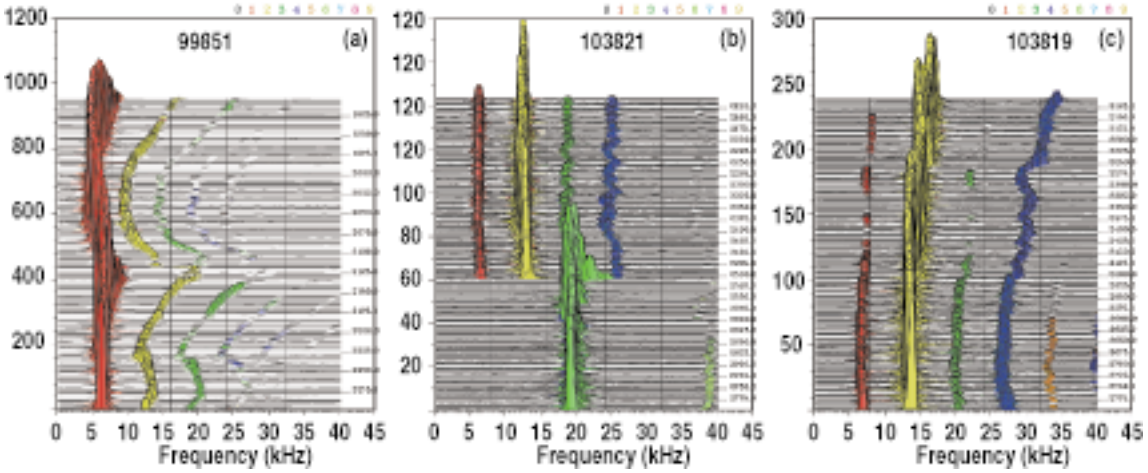

Fig. 5. Three examples of the variation of the mix of toroidal mode numbers n involved in the edge harmonic oscillation. (a) A case where n = 1 is the dominant mode with frequencies varying in time because of changing plasma conditions. (b) A case which initially exhibits n=1,2, 3 and 4 with n = 2 dominant which spontaneously changes to n=3 dominated. (c) A case with n= 2, 4 initially which then adds n = 1, 3 later on in the shot. Plots show frequency spectra from an outer midplane magnetic probe; each spectrum spans 10 ms and is separated from its neighbor by 5 ms. Color code for toroidal mode number is given at the top of the plot.

either low power cases where the plasma is near the boundary of the transition to ELMing behavior or cases where locked modes affect the overall plasma behavior.

By moving the plasma radially and scanning the plasma edge across the BES chords, we can determine the amplitude of the edge harmonic density oscillation as a function of position with respect to the plasma edge. In Fig. 6, we have replotted the data from this sweep as a function of position relative to the separatrix. The density oscillation clearly peaks on the separatrix and has a full width at half maximum of about 2 cm. Because of possible finite lifetime effects and the 1 cm spot size of the BES view in the plasma, this width must be taken as an upper limit. Thirty of the BES views are arranged in a 6 (radial) by 5 (poloidal) array at the plasma edge with 1.1 cm radial and 2.1 cm vertical spacing. Although not as detailed as the plot in Fig. 6, the radial profile at any given time from one radial row of that array shows the same features. The frequency and amplitude of the edge harmonic oscillation detected on the magnetic probes also does not change during the outer gap sweep. Both the observations suggest the value of the outer gap does not affect the oscillation's structure.

By using the poloidal and toroidal magnetic probe arrays on DIII-D, one can attempt to determine the poloidal mode number m associated with a given toroidal mode number n. This analysis is complicated by the strongly shaped plasma. Within those limitations, one can use the m/n ratio to estimate the safety factor q of the rational surface on which

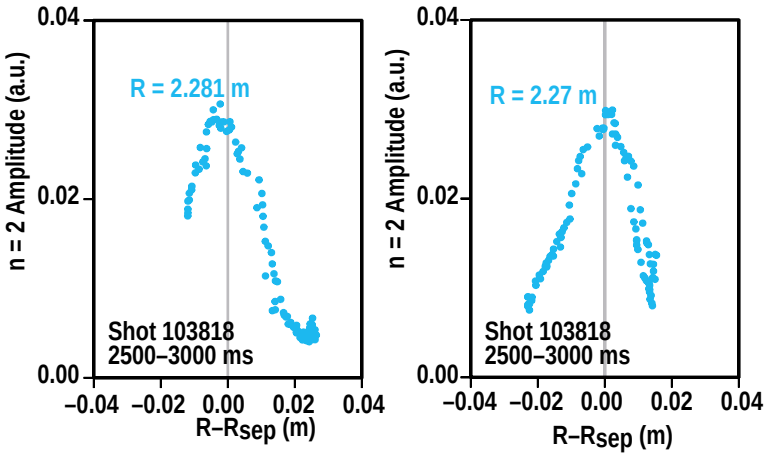

Fig. 6. Amplitude of density fluctuations from the beam emission spectroscopy system at the frequency of the n=2 toroidal mode number as a function of position relative to the separatrix. These data are produced by moving the edge of the plasma across the BES array and then replotting the data averaged over 10 ms intervals as a function of position relative to the separatrix at the outer midplane of the plasma. MHD equilibrium analysis using EFIT is employed to determine the separatrix location. The 10 ms averaging intervals are 50% overlapped so each point on the plot is 5 ms from its nearest neighbors. Data are shown for the complete sweep of the edge, both outwards and then inwards again. The agreement of the two parts of the sweep validates the assumption that there are no secular changes in the edge plasma over the time interval of the sweep. In addition, since the edge passes the two locations shown at different times, the agreement of the results from these two locations also rules out changes on a faster time scale.

conventional MHD mode analysis would suggest that the oscillation exists. Values between q = 3 and 4 are obtained in this way, for example, for the shot and time shown in Fig. 6. The q = 3 surface is 5 to 6 cm inside the separatrix while the q = 4 surface is 2 to 3 cm inside. Both of these locations are well inside the peak of the density oscillation shown in Fig. 6. There are no signatures in either the BES data or the ECE data indicating an MHD mode located at the q = 3 or 4 surfaces. The amplitude and relative phase of the oscillation varies smoothly across these positions. Whether the position inferred from the m/n ratio really has anything to do with the actual location of the oscillation in the plasma is not clear.

From fairly fundamental thermodynamic grounds, one expects plasma oscillations to extract free energy from plasma gradients. In an attempt to see which gradients might be important, we have plotted in Fig. 7 the oscillation amplitude from Fig. 6 and the profiles of a number of plasma parameters across the region near the plasma edge. From this plot, it appears that the radial electric field and the C^{6+} toroidal rotation are the quantities which have their maximum gradients closest to the peak of the density oscillation. The location of the peak of the ion temperature gradient is also fairly close to that location while the C^{6+} density gradient; electron density and electron temperature gradients peak further away. This leads us to speculate that the edge harmonic oscillation extracts its free energy from the rotation or electric field gradients. In assessing the location of the electron density and temperature measurements, one must have due regard for possible uncertainties caused by the need to use MHD equilibrium analysis to map the measurement from the upper outer edge of the plasma to the midplane. The ion measurements, BES measurement and electric

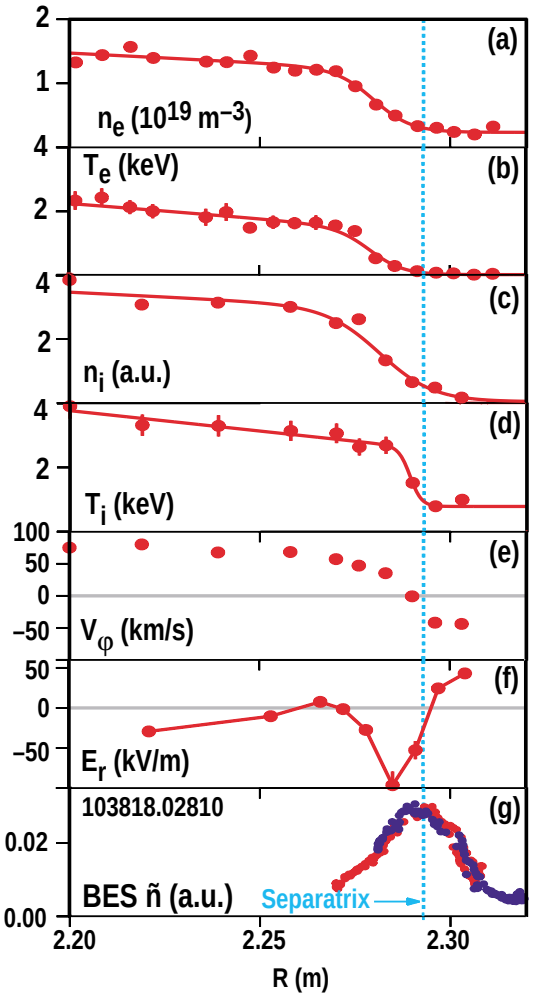

Fig. 7. Edge radial profiles of (a) electron density, (b) electron temperature, (c) C^{6+} density, (d) ion temperature, (e) C^{6+} toroidal rotation speed, (f) radial electric field and (g) BES amplitude from the two chords shown in Fig. 6. The profiles are taken at the time when the plasma edge reaches the maximum radius. The BES profiles are from the entire edge sweep, plotted relative to the separatrix location at the time all the other profiles were taken.

field measurement are not subject to these uncertainties because they are made on the plasma midplane.

The BES and the magnetic measurements can also be used to estimate the poloidal wavelength of the edge harmonic oscillation. By considering the phase shift along the poloidal direction of the BES two dimensional array, we find a wavelength of about 1 meter for the n = 2 harmonic. Because the BES array only spans 0.09 m in the poloidal direction, this wavelength measurement has essentially one significant digit. Similarly, using the poloidal phase shift on the magnetic probe array, we arrive at an estimate of about 1.3 m for the same n = 2 harmonic. Given the need to project the magnetic measurements 20 cm back to the plasma surface to do this analysis, the two poloidal wavelength values are in reasonable agreement.

The edge harmonic oscillation is quite obvious in counter injected discharges. Since its discovery [10,11], we have also noticed that a similar oscillation sometimes exists in low power co-injected H-mode discharges. This oscillation is only seen infrequently with co-injection but it appears to have the same multiharmonic character as with counter injection. Unlike the counter injected case where more power helps remove the ELMs and bring on the edge harmonic oscillation, for co-injection this oscillation is present most frequently at beam powers of 2.5 MW or less. All cases where we have seen the edge harmonic oscillation in co-injected discharges have large ELMs. There is as yet no sign of quiescent H-mode with co-injection. In counter injected shots, when the edge harmonic oscillation first turns on after an ELM, the frequency drops. However, for co-injected discharges, the frequency rises when the oscillation first turns on after an ELM. For both co- and counter-injected cases, the edge harmonic oscillation rotates toroidally in the same direction as the neutral beams.

F. ELM stabilization

A key question for the quiescent H-mode is: Why do the ELMs go away? At present, we do not have the final answer to this. We have examined several hypotheses and have found reasons to question all of them.

An early hypothesis was that the edge harmonic oscillation was so virulent that it lowered the edge pressure gradient below the value needed to create ELMs. However, the plots in Fig. 1(h) and in Fig. 2 show that the edge pressure gradient in the quiescent phase is at least as large as that in the ELMing phase. Accordingly, this hypothesis is not consistent with the data. If one thinks in terms of comparing the edge pressure gradient to some critical gradient [21], one must conclude that the stability boundary has moved because of some change in the edge plasma conditions. As is shown in Fig. 8, whatever

sets the edge stability boundary, it allows the edge pressure gradient in the quiescent phase of the discharge to increase with triangularity, just as the gradient does in ELMing H-mode [21]. During this triangularity scan, the plasma remains essentially ELM-free showing that the pressure gradient is being measured under quiescent conditions.

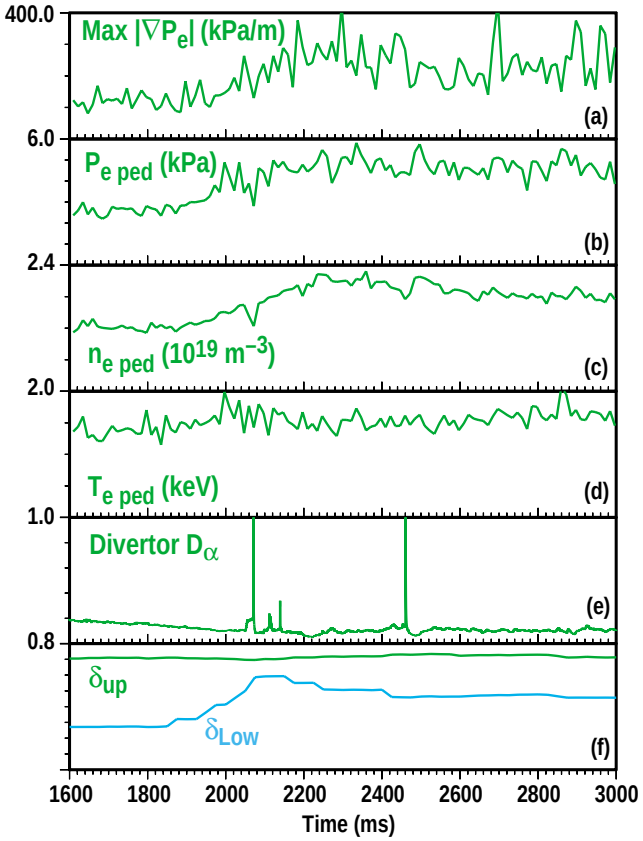

Fig. 8. Time variation of edge values as the lower triangularity of the discharge is varied at constant current (1.3 MA) and constant beam power (7.0 MW). (a) Maximum edge electron pressure gradient; pedestal values of (b) electron pressure, (c) electron density and (d) electron temperature; (e) divertor D_α emission, (f) upper and lower triangularity of the plasma. Values in (a-d) are determined from the hyperbolic fit to the Thomson scattering data. Notice that the maximum pressure gradient and the pedestal pressure both increase about a factor of 2.4 when the triangularity is increased.

Another hypothesis was that the edge harmonic oscillation represents the MHD precursor to an ELM which has been saturated by an unspecified mechanism at a level below that needed to cause the transient ergodization which gives the confinement degradation and consequent D_α burst associated with the fully developed ELM. There are certainly cases where the edge harmonic oscillation persists until an ELM occurs; this can happen, for example, after the edge harmonic oscillation has started but before the ELMs are completely suppressed. However, there are also a number of cases where the edge harmonic oscillation stops and an ELM does not take place for several tens of milliseconds. These cases were discussed in Section I.E. This behavior seems inconsistent with the concept of a precursor. It is a strange precursor which goes away well prior to the onset of the phenomenon which it is supposed to trigger.

Additional evidence against the idea that the edge harmonic oscillation is a saturated ELM precursor comes from the co-injection observations. As is common with co-injected plasmas, for these cases the ELM precursors are observed to rotate in the electron drift direction (opposite to the beam direction). The edge harmonic oscillation in both co- and counter-injection cases rotate in the direction of the neutral beams. This observation

strongly suggests that the edge harmonic oscillation and the ELM precursors are different modes.

G. Relationship to EDA operation in C-Mod

First discovered in 1996, EDA operation [7-9] in the C-Mod tokamak has some distinct similarities to the quiescent H-mode in DIII-D. In both cases, constant density operation is possible owing to the increase in particle transport caused by an edge oscillation. However, detailed comparison of the characteristics of the edge oscillation in the two machines shows distinct differences in its behavior. These are summarized in Table I. The most striking differences are in the frequency and poloidal wavelength of the two oscillations. In addition, although some magnetic component of the quasi-coherent mode in C-Mod has been seen by inserting magnetic probes into the scrape-off layer plasma, that magnetic component appears to be much weaker than that in the edge harmonic oscillation. Indeed, the edge harmonic oscillation was first observed using the magnetic probes on the DIII-D vessel wall and the associated density and temperature fluctuations were only seen much later.

Table I
Characteristics of Edge Oscillation in EDA and Quiescent H-mode

	Edge Harmonic Oscillation (DIII–D)	Quasi-Coherent Mode (C–Mod)
Increases D_α level in divertor	Yes	Yes
Increases particle transport across separatrix	Yes	Yes
Location	Foot of edge barrier	Edge density barrier
Frequency	6–10 kHz (n=1)	60–200 kHz
Toroidal mode number	Multiple, variable mix n=1–10	Unknown
Poloidal wavelength	~100 cm (m ~ 5)	~1 cm
Oscillations seen on	Magnetic probes at vessel wall	Magnetic probes in SOL
	BES, FIR, PCI, reflectometry, ECE, Langmuir probes in SOL and on divertor plate	PCI, reflectometry Langmuir probes just inside separatrix

III. QUIESCENT DOUBLE BARRIER OPERATION

One of the themes of advanced tokamak research on D III-D is understanding and control of core transport barriers. The goal is to optimize MHD stability and bootstrap current by adjusting barrier location and width [22,23]. Counter neutral beam injection was used in the 1999 campaign to broaden the core transport barrier [22,23]. This year, we discovered that the reduced transport core combines very naturally with the quiescent H-mode edge to produce long lasting quiescent double barrier plasmas which exhibit both core and edge transport barriers. The lack of ELMs in the quiescent H-mode means no degradation of the reduced transport core by pulsed, edge MHD events. In addition, counter neutral beam injection produces sufficient counter current drive on axis to hold the minimum q value significantly above one. This allows sawtooth-free operation which means no degradation of the reduced transport core due to sawteeth. As is shown in Fig. 9, we have produced discharges with $\beta_N H_{89}$ up to 7 which lasted for 5 τ_E. This $\beta_N H_{89}$ is substantially above the value of 4 usually seen in standard ELMing H-mode.

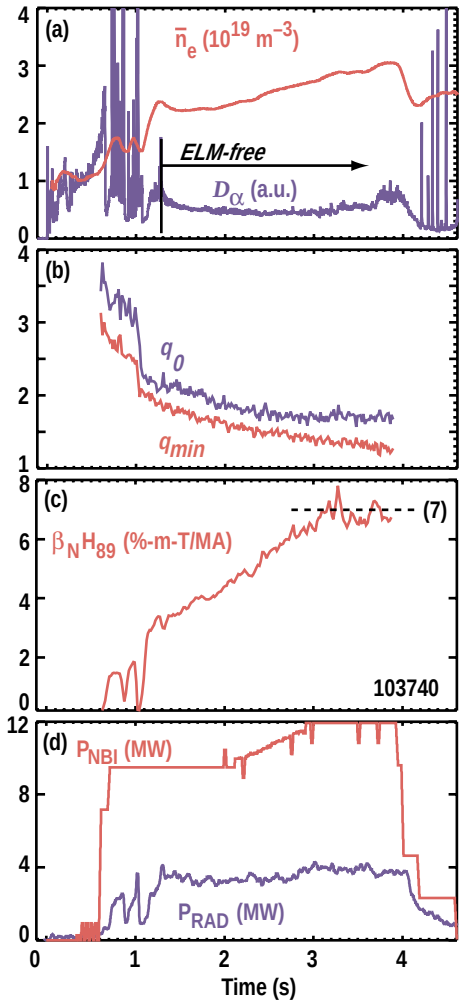

Fig. 9. Time history of one of the highest performance QDB discharges to date in DIII-D. (a) Line-averaged density and divertor D_α emission, (b) central safety factor q_0 and minimum safety factor q_{min}, (c) $\beta_N H_{89}$, (d) neutral beam input power and total radiated power. Toroidal field is 2.0 T and plasma current is 1.3 MA.

Since QDB plasmas were only recently discovered, we have not had time to optimize them fully. To date, we have achieved energy confinement times $\tau_E \leq 150$ ms, central ion temperatures $T_i(0) \leq 19$ keV, central electron temperatures $T_e(0) \leq 6$ keV, $\beta_N \leq 2.9$ and $H_{89} \leq 2.4$ in QDB plasmas. The behavior we have seen to date suggests that there is room to improve these parameters.

Most of the discharges already discussed in this paper have the reduced transport core. The core transport reduction improves with increasing input power, as can be seen by comparing the β_N H_{89} values in Fig. 9 to those in Fig. 1. This behavior is consistent with our expectations based on E×B shear stabilization of turbulence. A distinct advantage of working with the quiescent H-mode edge is that the shot lasts long enough that the power input can be ramped up slowly. This allows a gentle, gradual expansion of the reduced transport core. The core transport is sufficiently low in these discharges that an attempt to increase the input power quickly results in locally very steep pressure gradients which can lead to disruptions caused by violation of local MHD stability limits.

The advantage of the H-mode edge barrier for overall performance is shown in Fig. 10. The temperature profiles in the QDB case have increased over those in the L-mode edge case by a substantial, nearly constant offset due to the H-mode edge transport barrier. Fig. 10 also illustrates that the core and edge reduced transport regions do not merge; there is a flat spot in the profiles somewhat inside the edge. This can be understood from the model of E×B shear decorrelation of turbulence because the E_r profile [Fig. 10(c)] has a flat region around $\rho = 0.8$. Accordingly, E×B shear stabilization and the associated transport reduction should be absent here. This flat spot in the E_r

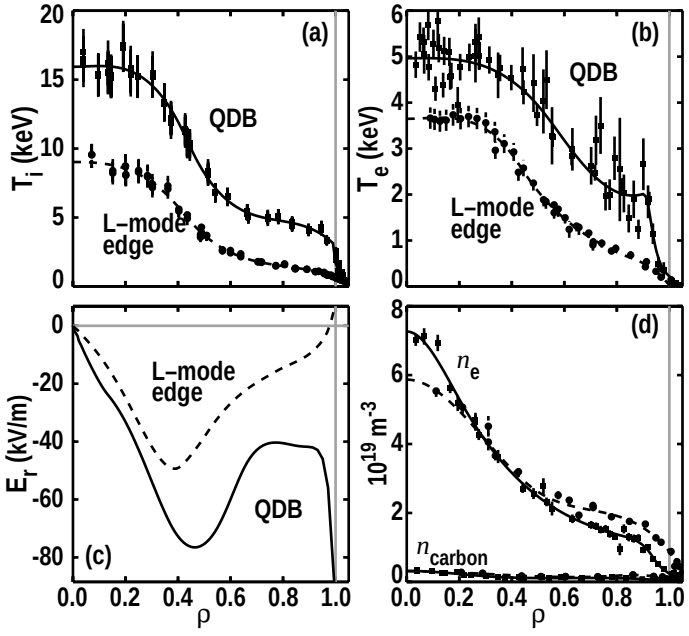

Fig. 10 Comparison of profiles for two plasma conditions with counter neutral beam injection; one has a reduced transport core with L-mode edge and the other is the QDB regime. (a) Ion temperature, (b) electron temperature, (c) radial electric field and (d) electron and C^{6+} density profile. Notice the increase in temperature through out the QDB plasma relative to the L-mode edge case caused by the edge transport barrier. Edge density in the QDB case is lower than that in the L-mode case because of cryopumping. L-mode edge ITB case is shot 99849 at 1.12 s while QDB case is shot 103740 at 3.3 s.

profile is a generic effect in counter injected H-mode discharges due to the negative E_r in the plasma core combined with the negative E_r well at the plasma edge.

Transport analysis shown in Fig. 11 confirms the qualitative impression from the profiles in Fig. 10. There is a substantial reduction in electron and ion thermal diffusivities in the core of these discharges. The ion thermal diffusivity is at or below the standard, Chang-Hinton neoclassical level [24]. The transport reduction around $\rho = 0.8$ to 0.9 is minor, as expected from the flat spot in the E_r profile.

Data from our FIR scattering system [18] indicates that broadband turbulence is reduced across most of the plasma throughout the QDB phase of these discharges compared to what is seen in discharges with a reduced transport core but an L-mode edge. This is consistent with the picture of core transport reduction through E×B shear decorrelation of turbulence [22,25]. Additional evidence consistent with this model comes from measurements of the radial correlation length of the turbulence from correlation reflectometry [16]. As is shown in Fig. 12(a), in L-mode plasmas, the measured radial correlation length tracks the $\rho_{\theta,s}$ fairly well. It also compares well with 5-8 times ρ_s. Here, $\rho_{\theta,s}$ and ρ_s are the poloidal and toroidal ion gyroradii, respectively, but evaluated using the local electron temperature. However, in the QDB plasmas, Fig. 12(b) shows a substantial reduction in the correlation length in the plasma core relative to $\rho_{\theta,s}$. The reduction factor is smaller in the outer region of the plasma. Since one expects the radial correlation length to be the step size for turbulent transport, the change in this ratio with radius is qualitatively consistent with the increase in transport with radius.

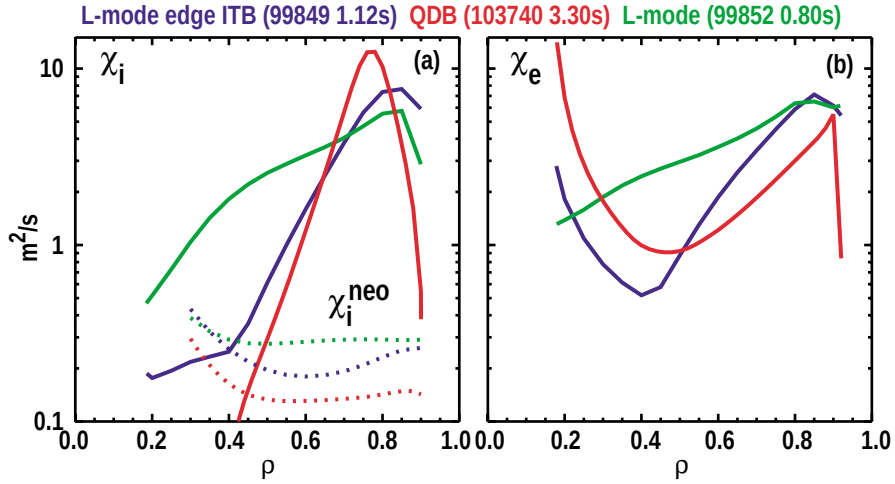

Fig. 11. (a) Ion and (b) electron thermal diffusivities for three cases: L-mode plasma, reduced transport core with L-mode edge and reduced transport core with quiescent H-mode edge (QDB).

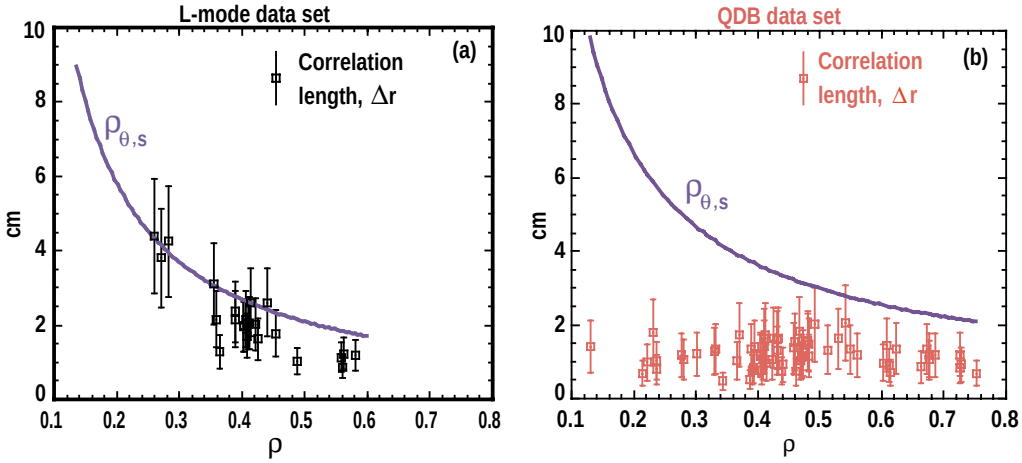

Fig. 12. Radial correlation length of the turbulent density fluctuations measured by correlation reflectometry compared with $\rho_{\theta,s}$, the poloidal ion gyroradius evaluated using the electron temperature. (a) An L-mode case in which the measured radial correlation length matches $\rho_{\theta,s}$ well, (b) a QDB case showing the radial correlation length decreasing to values much smaller than $\rho_{\theta,s}$ over most of the plasma.

IV. CONCLUSIONS

By utilizing counter neutral beam injection plus density reduction through cryopumping, we have produced quiescent double barrier plasmas in DIII-D with performance substantially improved over that in standard ELMing H-mode. These discharges have an ELM-free, quiescent H-mode edge with no D_α bursts and no pulsed heat load to the divertor. Edge particle transport in this regime is sufficiently rapid that discharges can be operated with constant density and constant radiated power in spite of the absence of ELMs. In addition, reduced transport core plasmas fit quite naturally with the quiescent H-mode edge owing to the lack of ELMs and absence of sawteeth. Provided enough off-axis co-current drive can be provided to keep the minimum q above one, such shots look like they could be run in steady state.

In the early 1990's, reduced core transport plasmas were seen only in transient conditions. One of the goals of DIII-D research over the past five years has been to extend the duration of such plasmas. With the QDB regime, we have pushed the duration to >3.5 seconds or about 25 τ_E. It now appears that the only obstacle to operating such plasmas in steady state is the need for sufficient current drive to keep minimum q above one.

A key issue for future research is acquiring the understanding needed to utilize the quiescent H-mode in a tokamak reactor environment. If this can be done, such plasmas would be a reactor designer's dream. They solve the pulsed divertor heat load problem posed by ELMs. In addition, they are compatible with reduced core transport regions needed for advanced tokamak operation.

REFERENCES

[a)]University of Texas, Austin, Texas.
[b)]University of California, Los Angeles, California.
[c)]University of Wisconsin, Madison, Wisconsin.
[d)]Max Planck Institut fur Plasmaphysik, Garching, Germany.
[e)]Lawrence Livermore National Laboratory, Livermore, California.
[f)]University of California, San Diego, California.
[g)]Massachusetts Institute of Technology, Cambridge, Massachusetts.
[h)]Princeton Plasma Physics Laboratory, Princeton, New Jersey.
[i)]Oak Ridge National Laboratory, Oak Ridge, Tennessee.
[j)]Sandia National Laboratories, Albuquerque, New Mexico.

[1] ITER Physics Basis Document, Nucl. Fusion **39**, 2137 (1999).
[2] T.S. Taylor, H.E. St John, A.D. Turnbull, Y.R. Lin-Liu, K.H. Burrell, V.S. Chan, M.S. Chu, J.R. Ferron, L.L. Lao, R.J. LaHaye, E.A. Lazarus, R.L. Miller, P.A. Politzer, D.P. Schissel, E.J. Strait, Plasma Phys. and Contro. Fusion Research **36**, B229 (1994).
[3] T.S. Taylor, Plasma Phys. and Contr. Fusion **39**, B47 (1997).
[4] A.W. Leonard, A. Hermann, K. Itami, J. Lingertat, A. Loarte, T.H. Osborne, W. Suttrop, J. Nucl. Mater. **266-269**, 100 (1999).
[5] K.H. Burrell, Rev. Sci. Instrum. **72** (2001) (to be published).
[6] J.L. Luxon, P. Anderson, F. Baity, C.B. Baxi, G. Bramson, N.H. Brooks, B. Brown, B. Burley, K.H. Burrell, R.W. Callis, G. Campbell, T.N. Carlstrom, A.P. Colleraine, J. Cummings, L. Davis, J.C. DeBoo, S. Ejima, R. Evanko, H. Fukumoto, R. Gallix, J. Gilleland, T. Glad, P. Gohil, A. Gootgeld, R.J. Groebner, S. Hanai, J. Haskovec, E. Heckman, M. Heiberger, F.J. Helton, N. Hosogane, C.-L. Hsieh, G.L. Jackson, G. Jahns, G. Janeschitz, E. Hohnson, A.G. Kellman, J.S. Kim, J. Kohli, A. Langhorn, L.L. Lao, P. Lee, S. Lightner, J. Lohr, M.A. Mahdavi, M. Mayberry, B. McHarg, T. McKelveny, R.L. Miller, C.P. Moeller, D. Moore, A. Nerem, P. Noll, T. Ohkawa, N. Ohyabu, T.H. Osborne, D.O. Overskei, P.I. Petersen, T.W. Petrie, J. Phillips, R. Prater, J. Rawls, E.E. Reis, D. Remsen, P. Riedy, P. Rock, K.M. Schaubel, D.P. Schissel, J.T. Scoville, R. Seraydarian, M. Shimada, T. Shoji, B. Sleaford, J.P. Smith, Jr., P. Smith, T. Smith, R.T. Snider, R.D. Stambaugh, T.S. Taylor, J. Tooker, M. Tupper, S.K. Wong, S. Yamaguchi, Plasma Phys. and Contr.

Nucl. Fusion Research 1986 (International Atomic Energy Agency, Vienna, 1987) Vol. I, p. 159.

[7] M. Greenwald, R. Boivin, P. Bonoli, R. Budny, C. Fiore, J. Goetz, R. Granetz, A. Hubbard, I. Hutchinson, J. Irby, B. LaBombard, Y. Lin, B. Lipschultz, E. Marmar, A. Mazurenko, D. Mossessian, T. Sunn Pedersen, C.S. Pitcher, M. Porkolab, J. Rice, W. Rowan, J. Snipes, G. Schilling, Y. Takase, J. Terry, S. Wolfe, J. Weaver, B. Welch, and S. Wukitch, Phys. Plasmas **6**, 1943 (1999).

[8] M. Greenwald, R. Boivin, P. Bonoli, C. Fiore, J. Goetz, R. Granetz, A. Hubbard, I. Hutchinson, J. Irby, Y. Lin, E. Marmar, A. Mazurenko, D. Mossessian, T. Sunn Pedersen, J. Rice, J. Snipes, G. Schilling, J. Snipes, G. Taylor, J. Terry, S. Wolfe, and S. Wukitch, Plasma Phys. and Contr. Fusion **42**, A263 (2000).

[9] A. Hubbard, et al., Phys. Plasmas **8**, (2001) (to be published) this conference.

[10] K.H. Burrell, C.M. Greenfield, W.P. West, M.R. Wade, J.C. Rost, Bull. Am. Phys. Soc. **44**, 127 (1999).

[11] R.J. Groebner, D.R. Baker, K.H. Burrell, T.N. Carlstrom, J.R. Ferron, P. Gohil, L.L. Lao, D.M. Thomas, T.H. Osborne, W.P. West, "Progress in Quantifying the Edge Physics of the H–mode Regime in DIII–D," to be published in Nucl. Fusion.

[12] G.L. Jackson, J. Winter, T.S. Taylor, C.M. Greenfield, K.H. Burrell, T.N. Carlstrom, J.C. DeBoo, E.J. Doyle, R.J. Groebner, L.L. Lao, C.L. Rettig, D.P. Schissel, E.J. Strait, and the DIII-D Research Team, Phys. Fluids **B4**, 2181 (1992).

[13] J.G. Watkins, J. Salmonson, R.A. Moyer, R. Doerner, R. Lehmer, L Schmitz, and D.N. Hill, Rev. Sci. Instrum. **63** (10) 4728-4730.

[14] D. Buchenauer, W.L. Hsu, J.P. Smith, D.N. Hill, Rev. Sci. Instrum. **61**, 2873 (1990).

[15] G.R. McKee, R. Ashley, R. Durst, R. Fonck, M. Jakubowski, K. Tritz, K.H. Burrell, C.M. Greenfield, and J.I. Robinson, Rev. Sci. Instrum **70**, 913 (1999).

[16] T.L. Rhodes, et al., Plasma Phys. Control Fusion **40**, 1575 (1998).

[17] E.J. Doyle, et al., Plasma Phys. Contr. Fusion **42**, A237 (2000).

[18] C.L. Rettig, S. Burns, R, Philipona, W.A. Peebles, N.C. Luhmann, Jr., Rev. Sci Instrum. **61**, 3010 (1990).

[19] S. Coda, M. Porkolab, and T.N. Carlstrom, Rev. Sci. Instrum. **63**, 4974 (1992).

[20] Z. Wang, J. Lohr, G.L. Bell, C. Hsieh, J. Luo, R.E. Stockdale, J.B. Wilgen, and J. Zhang, Proc. 9th Workshop on Electron Cyclotron Emission and Electron Cyclotron Heating, Borrego Springs, California, 1995, (World Scientific Publishing, Singapore, 1995) p.427.

[21] J.R. Ferron, M.S. Chu, G.L. Jackson, L.L. Lao, R.L. Miller, T.H. Osborne, P.B. Snyder, E.J. Strait, T.S. Taylor, A.D. Turnbull, A.M. Garofalo, M.A. Makowski, B.W. Rice, M.S. Chance, L.R. Baylor, M. Murakami, and M.R. Wade, Phys. Plasmas **7**, 1976 (2000).

[22] C.M. Greenfield, J.C. DeBoo, T.C. Luce, B.W. Stallard, E.J. Synakowski, L.R. Baylor, K.H. Burrell, T.A. Casper, E.J. Doyle, D.R. Ernst, J.R. Ferron, P. Gohil, R.J. Groebner, L.L. Lao, M.A. Makowski, G.R. McKee, M. Murakami, C.C. Petty, R.I. Pinsker, P.A. Politzer, R. Prater, C.L. Rettig, T.L. Rhodes, B.W. Rice, G.L. Schmidt, G.M. Staebler, E.J. Strait, D.M. Thomas, and M.R. Wade, DIII-D Team, Phys. Plasmas **7**, 1959 (2000).

[23] E.J. Doyle, C.M. Greenfield, M.E. Austin, L.R. Baylor, K.H. Burrell, T.A. Casper, J.C. DeBoo, D.R. Ernst, C. Fenzi, P. Gohil, R.J. Groebner, W.W. Heidbrink, G.L. Jackson, T.C. Jernigan, J.E. Kinsey, L.L. Lao, M. Makowski, G.R. McKee, M. Murakami, W.A Peebles, R. Prater, C.L. Rettig, T.L. Rhodes, J.C. Rost, G.M. Staebler, B.W. Stallard, E.J. Strait, E.J. Synakowski, D.M. Thomas, M.R. Wade, R.E. Waltz, and L. Zeng, "Progress Towards Increased Understanding and Control of Internal Transport Barriers on DIII-D," Proc. of 18th IAEA Fusion Energy Conf., Sorrento, Italy, 2000 (International Atomic Energy Agency, Vienna) to be published in Nucl. Fusion.

[24] C.S. Chang and F.L. Hinton, Phys. Fluids **25**, 1493 (1982).

[25] K.H. Burrell, Phys. Plasmas **6**, 4418 (1999).

ACKNOWLEDGMENT

This work was supported by the U.S. Department on Energy under Contract Nos. DE-AC03-99ER54463, W-7405-ENG-48, DE-AC02-76CH03073, DE-AC05-00OR22725, DE-AC04-94AL85000, and Grant Nos. DE-FG03-97ER54415, DE-FG03-86ER53225, DE-FG03-96ER54373, DE-FG03-95ER54294, and DE-FG02-94ER54235.